Spin-valley entangled quantum Hall states in graphene

Nikolaos Stefanidis [1,*] and Inti Sodemann Villadiego [2,†]
[1] *Max-Planck-Institut für Physik komplexer Systeme, Dresden 01187, Germany*
[2] *Institut für Theoretische Physik, Universität Leipzig, D-04103, Leipzig, Germany*

(Received 17 September 2023; accepted 28 November 2023; published 12 December 2023)

We investigate interaction-driven integer quantum Hall states realized in Landau levels of monolayer graphene when two out of its four nearly degenerate spin-valley flavors are filled. By employing a model that accounts for interactions beyond pure δ-functions as well as Zeeman and substrate-induced valley potentials, we demonstrate the existence of a delicate competition of several phases with spontaneous generation of spin-valley entanglement, akin to the spontaneous appearance of spin-orbit coupling driven by interactions. We encounter a particular phase that we term the entangled-Kekulé-antiferromagnet (E-KD-AF) which only becomes spin-valley entangled under the simultaneous presence of Zeeman and substrate potentials, because it gains energy by simultaneously canting in the spin and valley spaces, by combining features of a canted antiferromagnet and a canted Kekulé state. We quantify the degree of spin-valley entanglement of the many competing phases by computing their bipartite concurrence.

DOI: 10.1103/PhysRevB.108.235137

I. INTRODUCTION

The phase diagram of monolayer graphene in strong magnetic fields continues to present puzzles. At charge neutrality in the $N = 0$ Landau level it is still debated whether graphene is in a Canted Antiferromgnet (CAF), as proposed in transport and magnon transmission experiments [1–5], or in a Kekulé (KD) state as visualized in STM experiments [6–9]. In higher Landau levels the nature of states remains much less clear and the experimental evidence much more limited [10].

Reference [11] introduced an important model that simplified the understanding of symmetry broken states relative to earlier studies [12–16] by capturing the valley symmetry breaking interactions in the $N = 0$ Landau level as pure δ function interactions. Recent studies, however, have emphasized the need to consider interactions beyond δ functions in higher Landau levels [10,17], and also in the $N = 0$ Landau level arising from Landau level mixing [18,19]. Also, in bilayer graphene with four mini-Dirac points per spin/valley induced by trigonal warping, lead to a rich quantum Hall problem analogous to having effective flavor-dependent interactions with finite range [20]. In this work we investigate the interplay of such longer range interactions with the presence of spin Zeeman and substrate-induced sub-lattice symmetry breaking potentials, within a model that is applicable to integer quantum Hall states of graphene in any of its Landau levels. We will demonstrate that the combination of these ingredients leads to an interesting competition of phases with spontaneous spin-valley entanglement. Interestingly we find a state which becomes entangled only under the simultaneous presence of spin and valley Zeeman terms and interactions with longer range than pure δ functions, which we term the Entangled-Kekulé-Antiferromagnet state (E-KD-AF) (see Fig. 1).

*nikos@pks.mpg.de
†sodemann@uni-leipzig.de

II. MODEL, MEAN-FIELD THEORY, AND ENTANGLEMENT MEASURE

A series of recent works have considered the following continuum model of the projected interaction Hamiltonian onto the nth Landau level of graphene [17–19,21]:

$$\mathcal{H}^N = \sum_{i<j} \{V_z^N(r_{ij})\tau_z^i\tau_z^j + V_\perp^N(r_{ij})\tau_\perp^i\tau_\perp^j\} - \epsilon_Z \sum_i s_z^i - \epsilon_V \sum_i \tau_z^i, \tag{1}$$

where $V_{z,\perp}^N(r_{ij})$ are interactions that depend only on distance r_{ij} between particles i, j, $\tau_\perp^i\tau_\perp^j = \tau_x^i\tau_x^j + \tau_y^i\tau_y^j$ and s_a, τ_a, $a = 0, \dots, 3$ are the Pauli matrices acting on the valleys and spin, respectively. This model captures the symmetry breaking terms beyond the $SU(4)$ invariant long-range part of the Coulomb interaction. This model goes beyond the model of Ref. [11] which can be viewed as a limit of Eq. (1) when the interactions become δ functions, $V_{z,\perp}(r_{ij}) = V_{z,\perp}\delta(r_i - r_j)$. References [1,17] have demonstrated that even for models of unprojected interactions that are short-ranged (see, e.g., Ref. [22]), effective interactions will naturally appear as a result of the projection onto higher Landau levels ($N \neq 0$). It has been also recently emphasized that corrections to pure delta functions appear naturally in higher Landau levels [17]

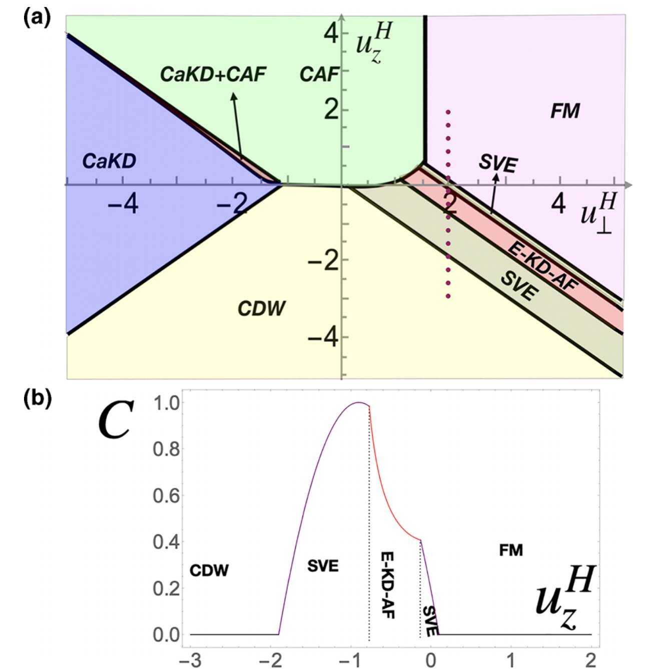

FIG. 1. (a) Integer quantum Hall states of half-filled Landau levels in graphene with Zeeman, $\epsilon_z = 1$, and valley potential, $\epsilon_v = 0.1$, and non-δ function interactions with $\Delta_\perp = 2$, $\Delta_z = 1$ [see Eq. (3)]. The spin-valley entangled state E-KD-AF appears between the two SVE states from Ref. [19]. (b) The concurrence (C) measure of spin-valley entanglement is plotted for the cut shown in (a) at $u_\perp^H = 2$.

by projecting the general model of short-distance interactions of graphene of Ref. [22], but can also appear even in the $N = 0$ Landau level (LL) due to Landau level mixing effects [18,19].

When there is an integer-filling of Landau levels, the Hartree-Fock variational energy functional of translationally invariant quantum Hall ferromagnets for the above model can be written as [17]

$$\mathcal{E}_{\rm HF}[P] = \frac{1}{2}\sum_{i=x,y,z}\left(u_i^H(\mathrm{Tr}\{\tau_i P\})^2 - u_i^X \mathrm{Tr}\{(\tau_i P)^2\}\right) - \epsilon_z \mathrm{Tr}\{s_z P\} - \epsilon_v \mathrm{Tr}\{\eta_z P\}. \quad (2)$$

Here, P is the projector into the occupied spinors, which in the case of half-filling (two filled components) equals $P = |F_1\rangle\langle F_1| + |F_2\rangle\langle F_2|$, where $|F_i\rangle$, $i = 1, 2$ are arbitrary orthonormal vectors within the four-dimensional Hilbert space of spin and valley flavors. Notice that the energy functional within Hartree-Fock theory does not depend on the detail form of the microscopic interactions but only on four independent interaction energy scales $u_z^H, u_z^X, u_x^{H,X} = u_y^{H,X} = u_\perp^{H,X}$, given by

$$u_a^H = \frac{V_a^N(\mathbf{q}=0)}{8\pi^2}, \quad u_a^X = \frac{1}{8\pi^2}\iint d\mathbf{q} V_a^N(\mathbf{q}), \quad a = \perp, z, \quad (3)$$

where $V_a^N(\mathbf{q})$ is the Fourier transform of the corresponding interaction term in Eq. (1). In the limit of pure δ function interactions, the difference between Hartree and exchange energy constants, $\Delta_{z,\perp} = u_{z,\perp}^H - u_{z,\perp}^X$ would vanish, and we would have only two interaction constants, as in the model of Ref. [11]. We will consider general spin-valley entangled variational states [17–19,21,23,24]:

$$|F\rangle_1 = \cos\frac{a_1}{2}|\boldsymbol{\eta}\rangle|\mathbf{s}\rangle + e^{i\beta_1}\sin\frac{a_1}{2}|-\boldsymbol{\eta}\rangle|-\mathbf{s}\rangle,$$
$$|F\rangle_2 = \cos\frac{a_2}{2}|\boldsymbol{\eta}\rangle|-\mathbf{s}\rangle + e^{i\beta_2}\sin\frac{a_2}{2}|-\boldsymbol{\eta}\rangle|\mathbf{s}\rangle. \quad (4)$$

Here, $|\boldsymbol{\eta}\rangle$ and $|\mathbf{s}\rangle$ are states parametrized by unit vectors $\boldsymbol{\eta}$ and $\mathbf{s}$ in the spin and valley Bloch spheres, respectively, and $a_{1,2}$ and $\beta_{1,2}$ are real constants. Because the projector P is effectively a mixed state, simple measures of bipartite entanglement applicable to pure states, such as the von Neumann entropy of the reduced density matrix, are not suitable. Instead, the degree of spin-valley bipartite entanglement associated with the projector P onto the above two states, can be measured by the concurrence C defined as [25,26]

$$C \equiv \mathrm{Max}\{\lambda_1 - \lambda_2 - \lambda_3 - \lambda_4, 0\}, \quad (5)$$

where λ_i are the eigenvalues of the matrix $R = P(\tau_y \bigotimes s_y)P^T(\tau_y \bigotimes s_y)P$, ordered according to $\lambda_i \geqslant \lambda_j$, for $i > j$. For projector onto the states in Eq. (4), the concurrence is

$$C = |\sin^2 a_1 - \sin^2 a_2|. \quad (6)$$

When the minima of HF energy are spin-valley disentangled states, we have $C = 0$, and these states can be separated into two classes, one of "valley-active" states with spinors given by

$$|F\rangle_1 = |\boldsymbol{\eta}_1\rangle|\mathbf{s}\rangle, \quad |F\rangle_2 = |\boldsymbol{\eta}_2\rangle|-\mathbf{s}\rangle, \quad (7)$$

where $\boldsymbol{\eta}_1, \boldsymbol{\eta}_2$ are two arbitrary directions in the valley Bloch sphere, and another class of "spin active" states, with spinors given by

$$|F\rangle_1 = |\boldsymbol{\eta}\rangle|\mathbf{s}_1\rangle, \quad |F\rangle_2 = |-\boldsymbol{\eta}\rangle|\mathbf{s}_2\rangle, \quad (8)$$

where $\mathbf{s}_1, \mathbf{s}_2$ are two arbitrary directions in the valley Bloch sphere.

In the limit of pure δ function interactions ($\Delta_{z,\perp} = 0$), Ref. [11] found a phase diagram with four spin-valley disentangled states that we reproduce in Fig. 2(a): FM (Ferromagnet), AF (Antiferromagnet), KD (Kekulé distortion), and CDW (Charge density wave). When interactions are not pure δ functions, and in the absence of Zeeman and valley potentials ($\epsilon_z = \epsilon_v = 0$), we recently found in Ref. [17] that a new phase termed the KD-AF (Kekulé- Antiferromagnet) can appear, as shown in Fig. 1(a). However in the absence of Zeeman and valley potentials ($\epsilon_z = \epsilon_v = 0$) all these five states have no spin-valley quantum entanglement. In particular, the KD-AF phase can be viewed as one of valley-active states from Eq. (7) having one component occupying an equal amplitude superposition of both valleys (e.g., $\boldsymbol{\eta}_1 = \hat{\boldsymbol{x}}$) with one spin and the other component occupying the opposite valley coherent superposition (e.g., $\boldsymbol{\eta}_2 = -\hat{\boldsymbol{x}}$) with the opposite spin, and therefore has a non-trivial spin-valley correlation, but no spin-valley entanglement properly speaking.

In this work, we will show that these five states (FM, AF, KD, CDW, KD-AF) can be viewed as parent states to several spin-valley entangled phases. Some of them, such as the

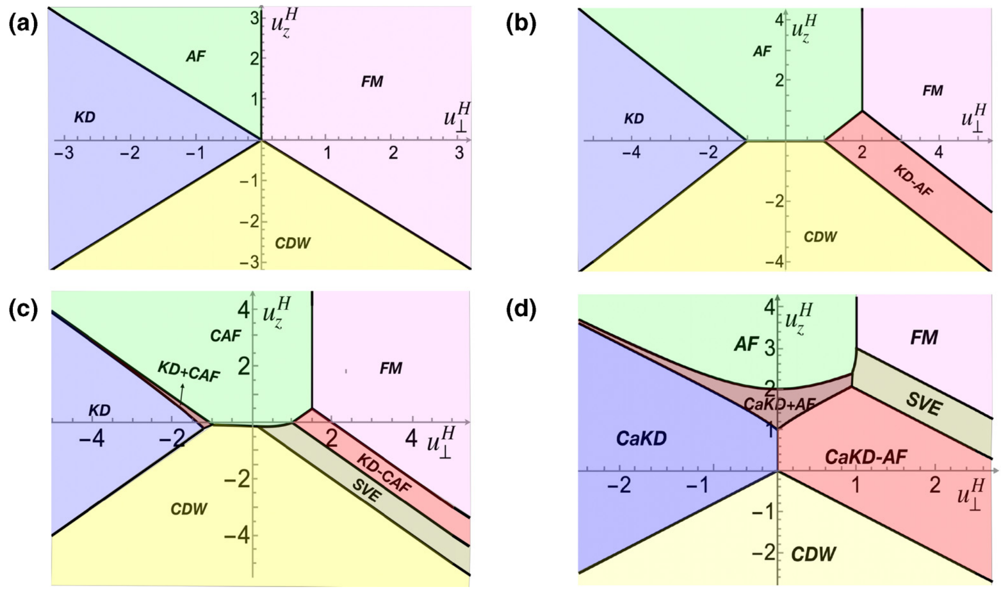

FIG. 2. Phase diagrams of integer quantum Hall states in graphene for half-filled Landau levels: (a) δ-function interactions and $\epsilon_z = \epsilon_v = 0$ from Ref. [11]. (b) For interactions with finite range, $\Delta_z = 1,\ \Delta_\perp = 2$, and $\epsilon_z = \epsilon_v = 0$, showing that the KD-AF becomes favorable. (c) For interactions with finite range, $\Delta_z = 1,\ \Delta_\perp = 2$, and $\epsilon_z = 1,\ \epsilon_v = 0$, showing that the KD-AF cants and becomes the KD-CAF and the SVE phase [19] becomes favorable. (d) For interactions with finite range, $\Delta_z = 2,\ \Delta_\perp = 1$, and $\epsilon_v = 1,\ \epsilon_z = 0$ showing that the KD-AF cants in the valleys space and becomes the CaKD-AF and the SVE phase of Ref. [19] appears in between the KD-AF and the FM states.

KD/AF coexistence and SVE states identified in Refs. [18,19], arise near the phase boundaries between these parent states after adding Zeeman and valley potentials. However, we will also show that among these five parent states the KD-AF is special because it is the only one that becomes spin-valley entangled under the simultaneous presence of Zeeman and valley sub-lattice potentials, and we will term the state that evolves continuously from the KD-AF under these perturbations the entangled-Kekulé-antiferromagnet (E-KD-AF) state (see Appendix S-VI in [27] for details of comparison with Ref. [19]).

A. Ground states with either Zeeman or valley potentials

We begin our analysis by studying the phase diagram when only the Zeeman coupling, $\epsilon_z \neq 0,\ \epsilon_v = 0$, is present in Eq. (1). We find that both the AF and the KD-AF cant their spins, which is a natural tendency of the anti-ferromagnetic states in order to take advantage of the Zeeman energy, evolving into the CAF and KD-CAF states depicted in Fig. 1(c). These two states remain, however, spin-valley disentangled. The KD-CAF appears in between the FM and the CDW as long as $0 < \epsilon_z < 2\Delta_z$.

However, as pointed out in Refs. [18,19], the CAF and the KD become unstable over some region close to their boundary leading to a mixed state of AFM-Kekulé phase coexistence which occupies a thin sliver of the phase boundary between these two phases. The analytic coordinates for this coexistence state are discussed in Appendix S-III in [27]. This phase coexistence occurs only when $\Delta_\perp > 0$ and otherwise there is a direct first order phase transition between the Kekulé and CAF states. Additionally, a finite ϵ_z induces the formation of another a new phase, the SVE of Ref. [19] growing from the boundary of the CDW with the KD-CAF. For $\epsilon_z = \epsilon_v = 0$ the SVE phase is never the ground state over any finite region, but interestingly it is is degenerate with KD-AF only at its boundaries with the FM and CDW. We note that the degeneracy at the boundary with the FM persists for all values of the Zeeman field, making this boundary presumably of higher symmetry [28]. When $\epsilon_z > 0$ and $\epsilon_v = 0$, the SVE, therefore, starts nucleating at the boundary of the CDW and the KD-AF and grows with increasing ϵ_z until it occupies the whole region between the CDW and the FM at a critical value of the Zeeman field $\epsilon_z^c = 2\Delta_z$. The transition of KD-CAF with the FM is continuous, i.e., the spin of the KD-CAF cants continuously until it reaches the fully polarized value of $s_z = 2$. The KD-CAF is therefore expected to have the similar signatures as the standard CAF state in spin sensitive probes, such as the magnon transmission experiments of Ref. [1].

It is also useful to consider the limit when ($\epsilon_v \neq 0$) is present but the Zeeman coupling vanishes ($\epsilon_z = 0$). This leads to the canting of the KD, similarly to the $N = 0$ Landau level, as discussed in Refs. [29] and also as shown in Fig. 2(d). Interestingly, since the KD-AF is simultaneously anti-ferromagnetic in the valley space and in the spin space, it will undergo canting of the valley pseudo-spins towards the z-axis driven by the finite ϵ_v. We also find that the ϵ_v also induces an intermediate coexistence region at the boundary between CaKD and AF analogous to the coexistence region of Refs. [18,19] [see Fig. 2(d)]. On the other hand, for $\epsilon_v > 0$ and $\epsilon_z = 0$, the SVE state now starts growing from the boundary of the FM with the KD-AF whereas the SVE is always degenerate with the KD-AF at its boundary with the CDW. The CaKD-AF persists until a critical value of the valley Zeeman, $\epsilon_v^c = 2\Delta_z$.

TABLE I. Competing states and their coordinates. The KD and KD-CAF are obtained by taking the limit of $\epsilon_v \to 0$ from the CaKD and CaKD-CAF, respectively, while the AF and CaKD-AF by taking the limit of $\epsilon_z \to 0$ from the CAF and CaKD-CAF, respectively. In the $a_{1,2}$ coordinates of E-KD-AF the $+$ $(-)$ sign corresponds to $a_1 (a_2)$.

States appearing for two filled Landau levels		
States	Coordinates	Concurrence C
CDW (Charge density wave)	$a_1 = a_2 = \theta_p = 0$	0
CaKD (Canted Kekulé distortion)	$a_1 = a_2 = 0,\ \theta_p = \cos^{-1}\left(\frac{\epsilon_v}{u_z^H - u_\perp^H + (\Delta_z - \Delta_\perp)}\right)$	0
FM (Ferromagnet)	$a_1 = 0,\ a_2 = \pi,\ \theta_p = \theta_s = 0$	0
CAF (Canted Antiferromagnet)	$a_1 = a,\ \cos a = -\frac{\epsilon_z}{2u_\perp^X,}\ a_2 = \pi - a,$ $\theta_p = \pi/2,\ \theta_s = 0,\ \beta = 0$	0
E-KD-AF (Entangled Kekulé distortion antiferromagnet)	$a_{1,2} = \cos^{-1}\{\pm\frac{\epsilon_z}{\Delta_\perp + \Delta_z - u_\perp^H - u_z^H} + \frac{\epsilon_v}{-\Delta_\perp + \Delta_z + u_\perp^H + u_z^H}\},$ $\theta_p = 0,\ \theta_s = 0,\ \beta = 0$	$\lvert \sin^2 a_1 - \sin^2 a_2 \rvert$
SVE (Spin-valley entangled phase of Ref. [19])	$a_1 = 0,\ \cos a_2 = \frac{\epsilon_z - \epsilon_v + u_z^H + u_\perp^H - \Delta_\perp}{-\Delta_z,}\ \theta_p = 0,\ \theta_s = 0,\ \beta = 0$	$\sin^2 a_2$

B. Ground states with both Zeeman and valley potentials

We now turn to the general case where both the Zeeman coupling and the hBN substrate are present. Our results are illustrated in Fig. 1(a). We again find a coexistence of the CaKD and the CAF along a sliver of the phase diagram. However, the main qualitative difference is that the KD-AF state transforms into a new spin-valley entangled state that we call the E-KD-AF when both spin and valley Zeeman fields are simultaneously present, as depicted in Fig. 1(b). This tendency originates from the fact that the KD-AF state gains energy by canting either in the spin and valley direction under the presence of spin or valley Zeeman terms, but it is impossible to construct disentangled states that cant simultaneously in this way (see Table I). We have found the exact coordinates of the spin-valley entangled minima of the Hartree-Fock functional in Eq. (2) and they satisfy $\beta = \theta_s = \theta_p = 0$, which is shared by all the phases in the right two quadrants of the phase diagrams. The E-KD-AF is now sandwiched between two spin-valley entangled SVE phases of Ref. [19] in the region between the FM and the CDW [see Fig. 1(a)], yet represents a qualitative distinct phase.

We can distinguish the two competing spin-valley entangled phases, namely the E-KD-AFM and the SVE of Ref. [19] by their order parameters, $\hat{O}_{ij} = Tr\{P\tau_i s_j\}$ (see Supplemental Material for further details [27]). Both of them have a vanishing total of valley and spin in the $x - y$ plane, $\hat{O}_{a0} = \hat{O}_{0a} = 0$, with $a = x, y$. However, the SVE phase of Ref. [19], has the order parameters $\hat{O}_{xx}, \hat{O}_{yy}$ locked to be equal $\hat{O}_{xx} = \hat{O}_{yy} = \sin a$, while for the E-KD-AF these order parameters are generally distinct and given by $\hat{O}_{xx} = \sin a_1 + \sin a_2$, $\hat{O}_{yy} = -\sin a_1 + \sin a_2$ (see Table I for the values of $a_{1,2}$). Moreover, as illustrated in Fig. 1(b), the concurrence of the SVE is different than that of the E-KD-AF (see also Table I). For a more detailed comparison of similarities and differences of our results with those of Ref. [19] see Sec. VI of the Supplemental Material [27].

III. SUMMARY AND DISCUSSION

We have studied the integer quantum Hall ferromagnet states of graphene within a model applicable to any of its Landau levels, and focused on the case of half-filling when two out of four of its nearly degenerate spin-valley states are filled. Our model accounts for valley symmetry-breaking interactions beyond pure δ functions, and includes the simultaneous presence of the Zeeman coupling and a substrate-induced valley symmetry breaking potential (e.g., from alignment with a hBN substrate). We have computed the concurrence measure of entanglement which allows us to quantify the degree of spin-valley entanglement of these states.

Besides the known spin-valley disentangled states such as the antiferromagnet and the Kekulé valence-bond solid, we have found a delicate competition of states featuring spontaneous spin-valley entanglement, akin to that arising from spin-orbit coupling, but whose origin stems purely from interaction driven spontaneous symmetry breaking. Notably, we have found a state which only becomes entangled under the simultaneous presence of spin and valley Zeeman terms and interactions with longer range than pure δ functions, which we term the Entangled-Kekulé-Antiferromagnet state (E-KD-AF). This tendency arises because this state combines features of the antiferromagnet and the Kekulé states, and the state tries to cant simultaneously in the spin and valley Bloch sphere in order to gain energy from these single particle terms, but it can only achieve this at the expense of becoming spin-valley entangled. An experimental technique to detect the Kekule-Antiferromagnetic states that we have discussed is spin-polarized STM [30], because in these states the Kekule bonds between between neighboring carbon atoms are opposite for spin up and spin down, and thus opposite Kekule bonding patterns between carbon atoms would appear in such spin-polarized STM.

ACKNOWLEDGMENTS

We would like to thank Ganpathy Murthy, Chunli Huang, and Nemin Wei for valuable discussions. N.S. acknowledges useful discussions with Panagiotis Giannakeas and Hongzheng Zhao. We acknowledge support by the Deutsche Forschungsgemeinschaft (DFG) through a research grant with Project No. 518372354.

[1] A. Young, J. Sanchez-Yamagishi, B. Hunt, S. Choi, K. Watanabe, T. Taniguchi, R. Ashoori, and P. Jarillo-Herrero, Tunable symmetry breaking and helical edge transport in a graphene quantum spin Hall state, Nature (London) **505**, 528 (2014).

[2] D. S. Wei, T. Van Der Sar, S. H. Lee, K. Watanabe, T. Taniguchi, B. I. Halperin, and A. Yacoby, Electrical generation and detection of spin waves in a quantum Hall ferromagnet, Science **362**, 229 (2018).

[3] H. Zhou, C. Huang, N. Wei, T. Taniguchi, K. Watanabe, M. P. Zaletel, Z. Papić, A. H. MacDonald, and A. F. Young, Strong-magnetic-field magnon transport in monolayer graphene, Phys. Rev. X **12**, 021060 (2022).

[4] A. K. Paul, M. R. Sahu, K. Watanabe, T. Taniguchi, J. Jain, G. Murthy, and A. Das, Electrically switchable tunneling across a graphene pn junction: Evidence for canted antiferromagnetic phase in $\nu = 0$ state, arXiv:2205.00710.

[5] P. Stepanov, S. Che, D. Shcherbakov, J. Yang, R. Chen, K. Thilahar, G. Voigt, M. W. Bockrath, D. Smirnov, K. Watanabe *et al.*, Long-distance spin transport through a graphene quantum Hall antiferromagnet, Nat. Phys. **14**, 907 (2018).

[6] A. Coissard, D. Wander, H. Vignaud, A. G. Grushin, C. Repellin, K. Watanabe, T. Taniguchi, F. Gay, C. B. Winkelmann, H. Courtois *et al.*, Imaging tunable quantum Hall broken-symmetry orders in graphene, Nature (London) **605**, 51 (2022).

[7] X. Liu, G. Farahi, C.-L. Chiu, Z. Papic, K. Watanabe, T. Taniguchi, M. P. Zaletel, and A. Yazdani, Visualizing broken symmetry and topological defects in a quantum Hall ferromagnet, Science **375**, 321 (2022).

[8] S.-Y. Li, Y. Zhang, L.-J. Yin, and L. He, Scanning tunneling microscope study of quantum Hall isospin ferromagnetic states in the zero Landau level in a graphene monolayer, Phys. Rev. B **100**, 085437 (2019).

[9] G. Farahi, C.-L. Chiu, X. Liu, Z. Papic, K. Watanabe, T. Taniguchi, M. P. Zaletel, and A. Yazdani, Broken symmetries and excitation spectra of interacting electrons in partially filled Landau levels, arXiv:2303.16993.

[10] F. Yang, A. A. Zibrov, R. Bai, T. Taniguchi, K. Watanabe, M. P. Zaletel, and A. F. Young, Experimental determination of the energy per particle in partially filled Landau levels, Phys. Rev. Lett. **126**, 156802 (2021).

[11] M. Kharitonov, Phase diagram for the $\nu = 0$ quantum Hall state in monolayer graphene, Phys. Rev. B **85**, 155439 (2012).

[12] K. Nomura and A. H. MacDonald, Quantum Hall ferromagnetism in graphene, Phys. Rev. Lett. **96**, 256602 (2006).

[13] M. O. Goerbig, R. Moessner, and B. Douçot, Electron interactions in graphene in a strong magnetic field, Phys. Rev. B **74**, 161407(R) (2006).

[14] J. Alicea and M. P. A. Fisher, Graphene integer quantum Hall effect in the ferromagnetic and paramagnetic regimes, Phys. Rev. B **74**, 075422 (2006).

[15] I. F. Herbut, Theory of integer quantum Hall effect in graphene, Phys. Rev. B **75**, 165411 (2007).

[16] J. Jung and A. H. MacDonald, Theory of the magnetic-field-induced insulator in neutral graphene sheets, Phys. Rev. B **80**, 235417 (2009).

[17] N. Stefanidis and I. S. Villadiego, Competing spin-valley entangled and broken symmetry states in the $N = 1$ Landau level of graphene, Phys. Rev. B **107**, 045132 (2023).

[18] A. Das, R. K. Kaul, and G. Murthy, Coexistence of canted antiferromagnetism and bond order in $\nu = 0$ graphene, Phys. Rev. Lett. **128**, 106803 (2022).

[19] S. J. De, A. Das, S. Rao, R. K. Kaul, and G. Murthy, Global phase diagram of charge-neutral graphene in the quantum Hall regime for generic interactions, Phys. Rev. B **107**, 125422 (2023).

[20] G. Murthy, E. Shimshoni, and H. A. Fertig, Spin-valley coherent phases of the $\nu = 0$ quantum Hall state in bilayer graphene, Phys. Rev. B **96**, 245125 (2017).

[21] J. Atteia, Y. Lian, and M. O. Goerbig, Skyrmion zoo in graphene at charge neutrality in a strong magnetic field, Phys. Rev. B **103**, 035403 (2021).

[22] I. L. Aleiner, D. E. Kharzeev, and A. M. Tsvelik, Spontaneous symmetry breaking in graphene subjected to an in-plane magnetic field, Phys. Rev. B **76**, 195415 (2007).

[23] Z. F. Ezawa, M. Eliashvili, and G. Tsitsishvili, Ground-state structure in $\nu = 2$ bilayer quantum Hall systems, Phys. Rev. B **71**, 125318 (2005).

[24] Y. Lian and M. O. Goerbig, Spin-valley skyrmions in graphene at filling factor $\nu = -1$, Phys. Rev. B **95**, 245428 (2017).

[25] A. Knothe and T. Jolicoeur, Edge structure of graphene monolayers in the $\nu = 0$ quantum Hall state, Phys. Rev. B **92**, 165110 (2015).

[26] F. Mintert, A. R. Carvalho, M. Kuś, and A. Buchleitner, Measures and dynamics of entangled states, Phys. Rep. **415**, 207 (2005).

[27] See Supplemental Material at http://link.aps.org/supplemental/10.1103/PhysRevB.108.235137 for a review of the projected model in the Nth Landau level and the Hartree-Fock theory, the linear stability analysis, and the concurrence of the states.

[28] F. Wu, I. Sodemann, Y. Araki, A. H. MacDonald, and T. Jolicoeur, SO(5) symmetry in the quantum Hall effect in graphene, Phys. Rev. B **90**, 235432 (2014).

[29] S. S. Hegde and I. S. Villadiego, Theory of competing charge density wave, Kekulé, and antiferromagnetically ordered fractional quantum Hall states in graphene aligned with boron nitride, Phys. Rev. B **105**, 195417 (2022).

[30] M. Bode, Spin-polarized scanning tunnelling microscopy, Rep. Prog. Phys. **66**, 523 (2003).